Synthesis and Proton-coupled Redox Properties of Mononuclear or Asymmetric Dinuclear Complexes of Ruthenium, Rhodium and/or Osmium containing 2,2'-Bis(2-pyridyl)-6,6'-Bibenzimidazole

Masa-aki Haga,*[a] Tomo-aki Ano,[a] Takahisa Ishizaki,[a] Kenji Kano,[b] Koichi Nozaki[c] and Takeshi Ohno[c]

[a] *Department of Chemistry, Faculty of Education, Mie University, 1515 Kamihama, Tsu, Mie, Japan*
[b] *Gifu Pharmaceutical University, 6-1 Mitahora-higashi 5, Gifu 502, Japan*
[c] *College of General Education, Osaka University, Toyonaka 560, Japan*

New mononuclear and heterodinuclear complexes, $[ML_2(H_2L^1)]^{2+}$ and $[L'_2M(H_2L^1)M'L''_2]^{4+}$ [M, M' = Ru, Rh and/or Os; L' or L'' = 2,2'-bipyridine (bipy), 1,10-phenanthroline or 4,4'-dimethylbipyridine], containing the dinucleating ligand 2,2'-bis(2-pyridyl)-6,6'-bibenzimidazole (H_2L^1) have been prepared. The metal-to-ligand charge-transfer bands are almost unaltered when changing from the mono- to di-nuclear complexes, indicating that the bridging H_2L^1 ligand has slightly lower π^* orbital energy than that of bipy. The bridging H_2L^1 ligand acts as a σ/π-donor ligand. Both the absorption spectra and the oxidation potentials of the complexes are strongly dependent on the solution pH, which determines the NH deprotonation of the co-ordinated ligand H_2L^1. The mononuclear complexes of Ru and Os act not only as basic acids but also as diacidic bases, while the heterodinuclear complexes essentially act as dibasic acids. The proton-coupled redox reaction was demonstrated by plots of $E_{\frac{1}{2}}$ *vs.* pH (Pourbaix diagrams). The pK_a values of the complexes reflect on both the type of metals and their oxidation states, M^{II} and M^{III}. The introduction of asymmetry in the dinuclear complexes containing H_2L^1 can provide not only a potential difference between the two metal sites but also a preferential protonation (or deprotonation) site.

The directional intramolecular electron-transfer process between metal ions in ligand-bridged di- or oligo-nuclear complexes has been much studied with regard to the design of photochemical molecular devices.[1] Recently, supramolecular assemblies comprised of oligonuclear metal complexes with different bridging ligands have been synthesised and proposed to have potential as building blocks for molecular level chips such as 'wires' and 'rectifiers'.[1b,2] The ruthenium–2,2'-bipyridine (bipy) chromophore is one of the promising building blocks for incorporation into a multicomponent system.[3]

Realizing the vectorial electron or energy transfer, asymmetric dinuclear metal complexes have received considerable attention.[4] The presence of asymmetry can provide a potential difference between the donor and acceptor sites and facilitate directed flow of electrons. From this point of view, we intend to synthesise a series of asymmetric di- and oligo-nuclear complexes with the combination of ruthenium, rhodium and osmium. Pyridine, pyrazine, pyrimidine or cyano groups have so far been used to bridge the ruthenium components in such complexes.[5] However, these have mainly π-acceptor properties. On the other hand, benzimidazole has a σ/π-donor property and furthermore possesses a dissociable NH proton.[6] Once the benzimidazole unit is co-ordinated to the metal ion the imino NH proton becomes more acidic and can easily be removed. The deprotonation of a bridging ligand may result in fairly large perturbations on the spectral and redox properties of dinuclear complexes.

Recently, we have prepared a new dinucleating compound, 2,2'-bis(2-pyridyl)-6,6'-bibenzimidazole (H_2L^1), and found that its complexes exhibited proton-induced switching of metal–metal interaction by proton transfer on the bridging L^1 ligand.[7] In order to extend the co-ordination chemistry of this new compound, a series of monomeric and asymmetric dinuclear complexes of Ru, Rh and Os containing L^1 are reported here,

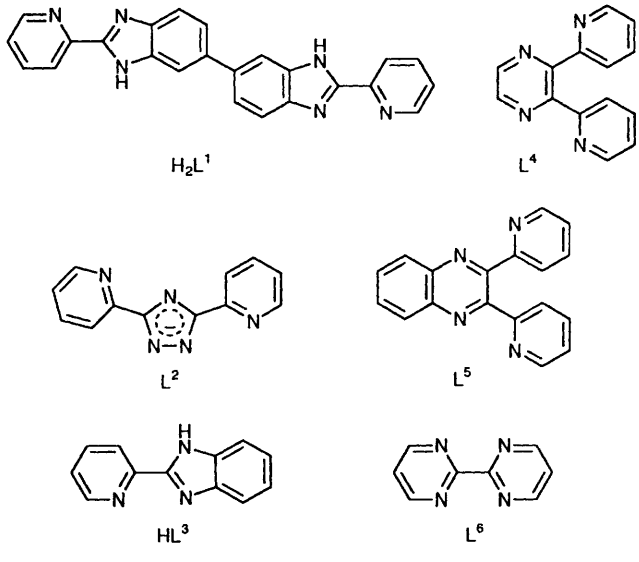

and the influence of pH on the absorption spectra and oxidation potentials is investigated in detail. The characteristics of L^1 will be compared to those of 3,5-bis(2-pyridyl)-1,2,4-triazole (L^2),[3i] 2,3-bis(2-pyridyl)pyrazine (L^4),[3c,o,q] 2,3-bis(2-pyridyl)-quinoxaline (L^5)[3f] or 2,2'-bipyrimidine (L^6).[3r]

Results and Discussion

Preparation and Characterization.—The compound H_2L^1 was obtained by the condensation reaction of 3,3'-diaminobenzidine with 2 equivalents of pyridine-2-carboxylic acid in

polyphosphoric acid.[7] Three geometrical isomers are anticipated as shown in Fig. 1, assuming free rotation about the biphenyl C–C bond. Only one group of signals for the ring protons and carbons can be observed in ^1H and ^{13}C NMR spectra in $(CD_3)_2SO$ after several recrystallizations from methanol. However, the ^1H NMR spectrum after the 1-methylation reaction of L^1 exhibits four *N*-methyl signals,[8] indicating the existence of three isomers of the 1,1'-dimethyl derivative (dmbpbim). Judging from these results, the rapid proton exchange at the NH imino group of H_2L^1 would render the three geometrical isomers equivalent, and only one set of NMR signals was observed. However, three geometries of H_2L^1 are fixed after co-ordination or N-methylation. A study of the separation of the geometrical isomers in dmbpbim is currently underway. In the present study, H_2L^1 was used after recrystallization twice.*

The stoichiometric reaction between $[ML'_2Cl_2]$ [L' = bipy, 4,4'-dimethyl-2,2'-bipyridine (dmbipy) or 1,10-phenanthroline (phen); M = Os, Rh or Ru] and H_2L^1 (1:1 molar ratio) proceeds smoothly in boiling ethanol–water. The mononuclear complex $[ML'_2(H_2L^1)][ClO_4]_2$ has been isolated as a perchlorate salt, and can be used as a starting material for synthesising di- or oligo-nuclear complexes. The dinuclear complexes were generally prepared by the reaction of $[M'L''_2Cl_2]$ (M' = Ru or Os, L'' = bipy or dmbipy) with $[ML'_2(H_2L^1)][ClO_4]_2$ in ethanol–water or ethylene glycol, depending on the metal M' and the ligand L''. The mono- or di-nuclear complexes were purified by Sephadex LH-20 column chromatography with methanol–acetonitrile or on SP Sephadex C-25 with acetonitrile–buffer. They possess several possible optical isomers based on the chirality of the octahedral metal centre (Λ and Δ) after the complexation of H_2L^1. All attempts to separate the isomers have so far failed.

The electrolyte type and molecular complexity of the cationic complexes can be discriminated by conductivity measurements. Experimentally, it has been shown that the slope of a $(\Lambda_o - \Lambda_e)$ *vs.* $c_e^{\frac{1}{2}}$ plot depends on the type of electrolyte, where Λ_o, Λ_e and c_e are the conductivity at infinite dilution, the equivalent conductivity, and the equivalent concentration, respectively.[9] A straight line was obtained for following complexes in acetonitrile at 20 °C (slope in mho $l^{\frac{1}{2}}$ equiv$^{-\frac{1}{2}}$): 2760 for $[(dmbipy)_2Ru(H_2L^1)Ru(phen)_2][ClO_4]_4$, 2450 for $[(bipy)_2Os(H_2L^1)Ru(bipy)_2][ClO_4]_4$, and 1150 for $[Ru(bipy)_2(H_2L^1)][ClO_4]_2$. The slope for a reference 2:1 electrolyte, $[Ru(bipy)_3][ClO_4]_2$, was 1350 mho $l^{\frac{1}{2}}$ equiv$^{-\frac{1}{2}}$ is close to that for the mononuclear complex. On the other hand, the slopes for the dinuclear complexes are twice as large as that for the mononuclear complex. Thus, these results indicate that the mono- and di-nuclear complexes are 2:1 and 4:1 electrolytes, respectively.

Absorption Spectra.—The spectral data for the mono- and di-nuclear complexes are collected in Table 1.

(*a*) *Mononuclear complexes.* The absorption spectrum of $[Ru(bipy)_2(H_2L^1)][ClO_4]_2$ consists of three well resolved bands. The band at 459 nm is assigned to the Ru^{II}–bipy and H_2L^1 metal-to-ligand charge transfer (m.l.c.t.) transition by comparison with the spectra of $[Ru(bipy)_3][ClO_4]_2$ and $[Ru(bipy)_2(HL^3)][ClO_4]_2$ [HL^3 = 2-(2-pyridyl)benzimidazole].[10] This assignment is supported by our recent results[11] from both transient absorption spectra and reduction potentials; *i.e.* the energy of the lowest unoccupied molecular orbital (LUMO) of the co-ordinated ligand is in the order $H_2L^1 \leqslant$ bipy ≈ phen < dmbipy. The m.l.c.t. band of $[Ru(bipy)_2(H_2L^1)][ClO_4]_2$ occurs at almost the same wavelength as that of $[Ru(bipy)_3][ClO_4]_2$ (452 nm). If H_2L^1 is a better σ donor than bipy, its ligand field will be stronger and the m.l.c.t. band should be at shorter wavelength; if it is a better π donor than bipy its ligand field is weaker and the m.l.c.t. band should be at longer wavelengths. Thus, the two effects appear nearly to cancel each other. Since free H_2L^1 has a π–π* intraligand transition at 337 nm (in MeCN), the band at 346 nm can be assigned to a π–π* (H_2L^1) intraligand transition. Although the m.l.c.t. transition of $[Ru(bipy)_2(H_2L^1)][ClO_4]_2$ occurs at almost the same energy as that of $[Ru(bipy)_2(HL^3)][ClO_4]_2$,[10] the π–π* ($H_2L^1$) transition occurs at lower energy compared to that of HL^3. This reflects the destabilization of the π orbital and the stabilization of the π* orbital based on the orbital interaction of two HL^3 chromophores. The higher band at 289 nm is assigned to the π–π* (bipy) intraligand transition. The corresponding osmium complex, $[Os(bipy)_2(H_2L^1)][ClO_4]_2$, has an additional absorption band at 606 nm, which can be assigned to a d_π–π* triplet transition. On the other hand, the absorption spectra of $[RhL'_2(H_2L^1)][ClO_4]_3$ (L' = bipy or phen) exhibit mainly ligand-based bands at around 310 [π–π* (bipy)] and 365 nm [π–π* (H_2L^1)] for L' = bipy, and 273 [π–π* (phen)] and 360 nm [π–π* (H_2L^1)] for L' = phen. The d–d transition seems to overlap the ligand-based transition.[3z,12]

(*b*) *Dinuclear complexes.* When the mononuclear complex, $[M(bipy)_2(H_2L^1)][ClO_4]_2$ (M = Ru or Os) is treated with another ruthenium or osmium centre to form dinuclear complexes the m.l.c.t. absorption maxima around 460 nm remain almost unaltered, except they become twice as intense compared to the mononuclear complexes (see Table 1). This is in sharp contrast to π-accepting bridging systems such as L^4, L^5 or L^6. A shift to longer wavelength of the m.l.c.t. band compared to that of the mononuclear complex has been reported when the latter containing such a π-accepting ligand forms a dinuclear complex.[3f,o,q,r] The energy of the π* orbital of the bridging ligand relative to bipy or phen determines the m.l.c.t. band energy. In the present H_2L^1 system, the energy of the π* orbital is slightly lower than that of bipy or phen.[11] Thus, the m.l.c.t. band energy is almost unaltered on going from the mono- to the di-nuclear complex.

Fig. 2 shows the absorption spectrum of $[(bipy)_2Ru(H_2L^1)Rh(bipy)_2][ClO_4]_5$ together with those of its monomeric components. The spectrum of this asymmetric dinuclear complex is essentially the sum of those of the components. The absorption spectrum of the Ru–Os dinuclear

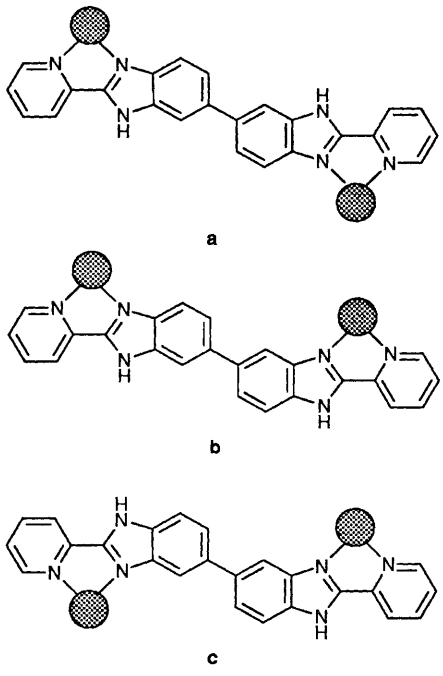

Fig. 1 Three possible geometrical isomers of H_2L^1, assuming free rotation about the C–C bond of the biphenyl moiety. The co-ordination mode is shown for each isomer

* Only one of the three isomers of H_2L^1 is presented in the Schemes and Figures in this paper.

Table 1 Visible-UV spectral data for mononuclear $[ML_2(H_2L^1)][ClO_4]_2$ and dinuclear $[L_2M(H_2L^1)M'L'_2][ClO_4]_n$ (n = 4 or 5) in MeCN–buffer (1 : 1 v/v) at pH 2.3

				λ_{max}/nm (ε/dm^3 mol^{-1} cm^{-1})			
M	M′	L	L′	π–π* (L or L′)	π–π* (H_2L^1)	$(d_\pi–\pi^*)^1$	$(d_\pi–\pi^*)^3$
(*a*) Mononuclear complexes							
Rh		bipy		307 (42 600) 319 (47 900)	365 (sh)		
Rh		phen		273 (64 700) 304 (26 660)	360 (sh)		
Ru		bipy		289 (79 900)	346 (37 900)	459 (15 300)	
Os		bipy		292 (79 700)	344 (43 200)	489 (13 600)	606 (3690)
(*b*) Dinuclear complexes							
Ru	Ru	bipy	bipy	289 (136 000)	355 (53 500)	459 (27 000)	
Ru	Ru	phen	phen	264 (189 000)	358 (49 200)	454 (32 900)	
Ru	Ru	phen	dmbipy	264 (117 000) 287 (111 000)	347 (55 000)	458 (31 300)	
Ru	Os	bipy	bipy	290 (131 000)	355 (52 500)	458 (23 300)	606 (3880)
Ru	Rh	bipy	bipy	290 (78 000) 307 (55 000) 318 (54 400)	363 (48 400)	464 (sh)	
Ru	Rh	dmbipy	phen	280 (69 000) 307 (sh)	355 (36 000)	464 (sh)	
Rh	Rh	phen	phen	273 (154 700) 303 (49 000)	353 (28 300) 378 (28 300)		
Os	Os	bipy	bipy	292 (131 000)	356 (51 200)	489 (23 400)	606 (6470)

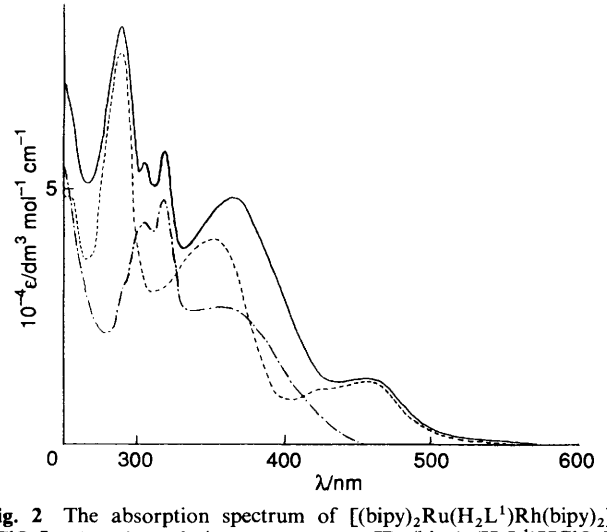

Fig. 2 The absorption spectrum of $[(bipy)_2Ru(H_2L^1)Rh(bipy)_2][ClO_4]_5$ (——) and its components $[Ru(bipy)_2(H_2L^1)][ClO_4]_2$ (– – – –) and $[Rh(bipy)_2(H_2L^1)][ClO_4]_3$ (— · —) in MeCN

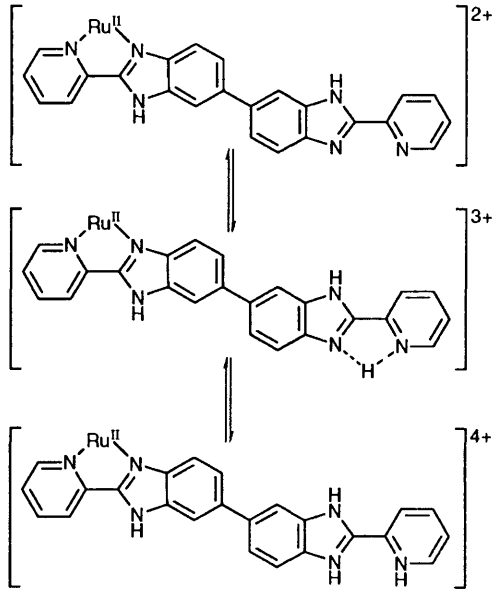

Scheme 1

complex is analogous. These results suggest that the metal–metal interaction in the ground state is small.

Acid–Base Equilibria of the Complexes from Spectrophotometric Studies.—The absorption spectra of the mono- and di-nuclear complexes in MeCN–buffer (1 : 1 v/v) are strongly dependent on the solution pH.

(*a*) *Mononuclear complexes.* An increase in pH for $[Ru(bipy)_2(H_2L^1)][ClO_4]_2$ leads to a decrease in the m.l.c.t. absorption intensity at 459 nm and at around 500 nm, while retaining the isosbestic points at 420 and 475 nm. The final spectrum at pH 10.65 returned to the original one after acidification, which indicates that the spectral changes are fully reversible. From these spectral changes, the acid dissociation constant, pK_a, was calculated to be 6.53. While H_2L^1 has two dissociable imino protons, the dissociation of only that attached to the co-ordinated benzimidazole moiety was observed in the range pH 2–12. This result is rationalized by the fact that the pK_a of the imino NH protons of free benzimidazole derivatives is usually around 14. On the other hand, the protonation of unco-ordinated nitrogens in the mononuclear H_2L^1 complex is also feasible (see Scheme 1). Above pH 2 a pH-dependent change in the absorption spectrum is observed, however the limiting spectrum could not be obtained even at pH 0. Thus, the pK_a value may be around or below 0. The pK_a value of $[Os(bipy)_2(H_2L^1)][ClO_4]_2$ (6.24) is a little smaller than that of the ruthenium analogue.

In the case of $[RhL'_2(H_2L^1)][ClO_4]_3$ the pK_a values of 2.82 (L′ = bipy) and 2.75 (L′ = phen) were obtained from the pH dependence of the absorption spectra. The large difference between the complexes of M^{II} (Ru or Os) and Rh^{III} is attributable to the stronger Lewis acidity based on the large positive charge on the metal ion, as pointed out previously.[13]

(*b*) *Dinuclear complexes.* For $[(bipy)_2Ru(H_2L^1)Os(bipy)_2][ClO_4]_4$ the absorption maxima at 458 and 606 nm were broadened on raising the solution pH, and the growth of a

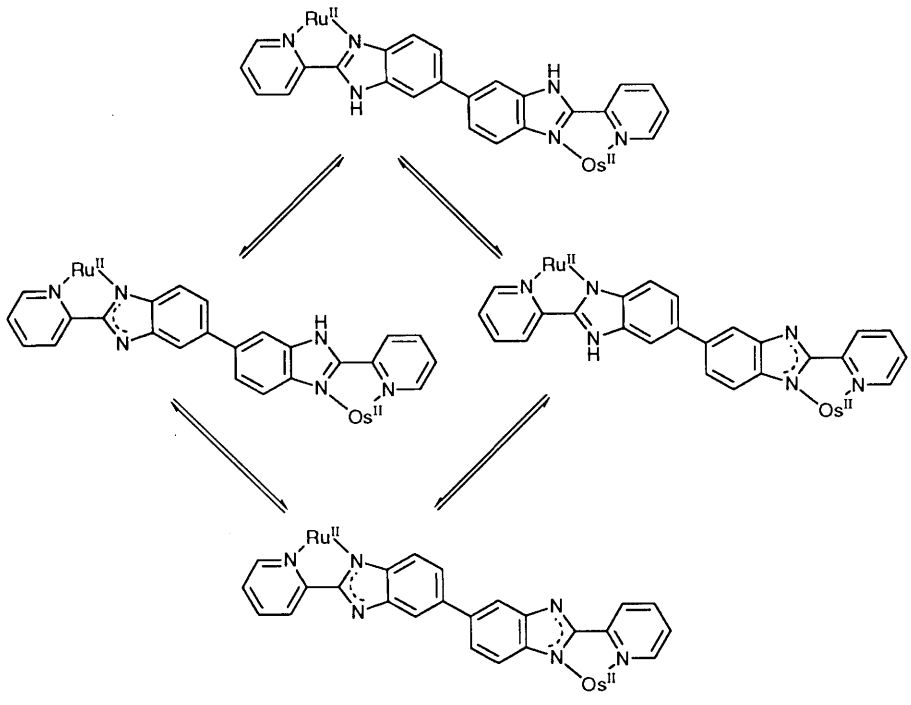

Scheme 2

shoulder at 485 nm and weak broad bands around 700 nm were observed. The absorbance *vs.* pH titration curve obtained from the spectral changes described above does not show any plateau in the middle pH region. The microscopic equilibria in Scheme 2 can be considered for this complex. The absence of supplementary information makes it difficult to determine the microscopic equilibrium constants quantitatively, and the present spectrophotometric titration is only capable of providing macroscopic equilibrium constants.† A non-linear regression analysis was carried out for the titration curve,[14] yielding macroscopic pK_a values of 5.10 and 6.53.

Fig. 3 shows the absorption spectra of heterodinuclear $[(bipy)_2Ru(H_2L^1)Rh(bipy)_2][ClO_4]_5$ in MeCN–buffer (1 : 1 v/v) as a function of pH. In the low pH region, changes in the band around 400 nm occur, arising from a H_2L^1 π–π^* ligand-localized transition. Further increase in pH leads to a decrease in the ruthenium-to-ligand m.l.c.t. band centred at 460 nm and an increase in the intensity of the band at 490 nm, and two well defined isosbestic points at 451 and 475 nm can be seen. The absorbance *vs.* pH curve for this spectrophotometric titration shows a clear plateau in the middle pH region, yielding macroscopic pK_a values of 2.25 and 6.27 (Fig. 4). In this complex the different oxidation states of the metal ions leads to a larger pK_a difference, $\Delta pK_a(=pK_{a2} - pK_{a1})$, compared to that of the Ru–Os complex. Thus, at least the predominant deprotonation site can be determined from these spectral changes; *i.e.* the first deprotonation occurs predominantly on the H_2L^1 co-ordinated to $Rh(bipy)_2$ and the second takes place on the $Ru(bipy)_2$ moiety.

The macroscopic acid-dissociation constants are collected in Table 2, together with those for homodinuclear complexes in MeCN–buffer (1 : 1 v/v)[7]

Proton-coupled Oxidative Electrochemistry.—(*a*) *Mononuclear complexes.* Electrochemical measurements provide information on the difference between the two oxidation states, *e.g.* Ru^{II} and Ru^{III}. In particular, the pK_a values for different oxidation states can be obtained by analysing plots of the standard redox potential $E^{o\prime}$ *vs.* pH (Pourbaix diagram). The

† The two tautomeric monoprotonated isomers in Scheme 2 are treated collectively as a single species.

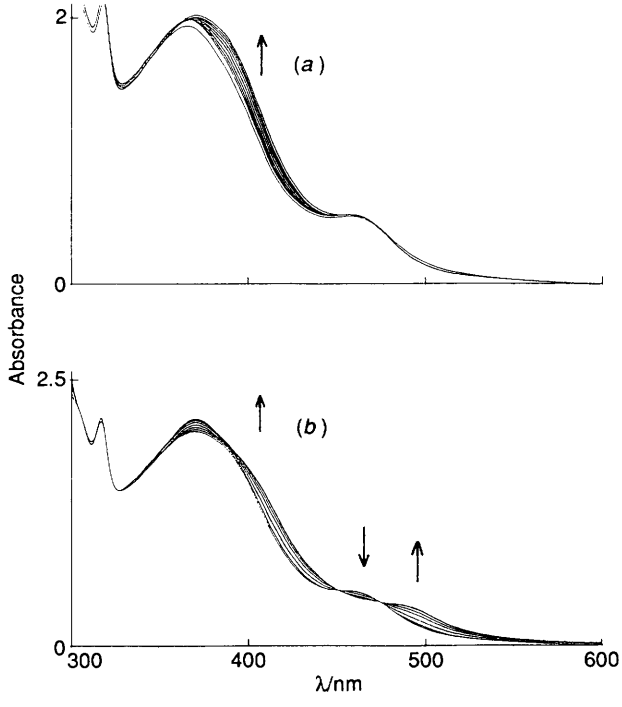

Fig. 3 Absorption spectra of $[(bipy)_2Ru(H_2L^1)Rh(bipy)_2][ClO_4]_5$ (6.6×10^{-5} mol dm^{-3}) at 20 °C in MeCN–buffer (1 : 1 v/v) at: (*a*) pH 2.60–5.30, (*b*) pH 5.30–8.00

cyclic voltammogram of $[Ru(bipy)_2(H_2L^1)][ClO_4]_2$ exhibits only one reversible wave in all the pH region examined here, while the position is strongly dependent on the pH. Fig. 5 shows the half-wave potential $E_{\frac{1}{2}}$ *vs.* pH for $[Ru(bipy)_2(H_2L^1)][ClO_4]_2$ in MeCN–buffer (1 : 1 v/v). The plot is composed of three straight-line segments with slopes of 0 (pH 0–1.6), −60 (1.6–7.0), and 0 mV per pH unit (7.0–12.0), respectively. Spectrophotometric study has revealed that this complex acts as a monobasic acid. Thus, the electrode process can be described as in Scheme 3 involving both redox and acid–base equilibria,

Table 2 Values of pK_a and electrode potentials (*vs.* Ag–AgCl) for mononuclear $[ML_2(H_2L^1)]^{n+}$ and dinuclear $[L_2M(H_2L^1)M'L_2]^{n+}$ in MeCN–buffer (1 : v/v)[a]

M	M'	L	L'	pK_{a1} or pK_{11}	pK_{a12}	pK_{a2} or pK_{21}	pK_{a22}	pK_{a31}	pK_{a32}
(*a*) Mononuclear complexes									
Rh		bipy		(2.82)					
Rh		phen		(2.75)					
Ru		bipy		7.0		1.6			
				(6.53)					
Os		bipy		6.7		2.4			
				(6.24)					
(*b*) Dinuclear complexes									
Ru	Ru	bipy	bipy[b]	5.8	8.1	1.4	6.9	1.0	2.0
				(5.61)	(7.12)				
Ru	Ru	phen	phen[b]	5.9	7.7	1.5	6.6	1.0	1.9
				(5.51)	(6.85)				
Ru	Ru	phen	dmbipy	6.5	7.4	2.0	6.7	1.0	2.4
				(5.31)	6.80)				
Ru	Os	bipy	bipy	5.6	6.9	2.8	6.4	1.4	2.8
				(5.10)	(6.53)				
Ru	Rh	bipy	bipy	2.3	6.7	1.4	2.3		
				(2.25)	(6.27)				
Ru	Rh	dmbipy	phen	2.8	6.6	2.0	2.8		
				(2.89)	(6.02)				
Rh	Rh	phen	phen	(< 0)	(2.67)				
Os	Os	bipy	bipy[b]	5.3	6.9	2.1	5.9	1.9	2.3
				(5.53)	(7.09)			(1.51)	(2.46)

M	M'	L	L'	E_1^0	E_2^0	E_3^0	E_4^0	E_5^0	E_6^0
(*a*) Mononuclear complexes									
Ru		bipy		0.96	0.64				
Os		bipy		0.59	0.34				
(*b*) Dinuclear complexes									
Ru	Ru	bipy	bipy[b]	0.94	0.98	0.72	0.97	0.65	0.73
Ru	Ru	phen	phen[b]	0.95	1.00	0.68	0.97	0.62	0.70
Ru	Ru	phen	dmbipy	0.86	0.97	0.62	0.91	0.55	0.67
Ru	Os	bipy	bipy	0.56	0.99	0.40	0.92	0.36	0.70
Ru	Rh	bipy	bipy	0.95	0.90	0.67			
Ru	Rh	dmbipy	phen	0.86	0.81	0.57			
Os	Os	bipy	bipy[b]	0.53	0.58	0.36	0.57	0.31	0.38

[a] The notations for the pK_a and E_n^0 values are defined in Schemes 3, 4 and 6. The values in parentheses were obtained spectrophotometrically. [b] Ref. 7.

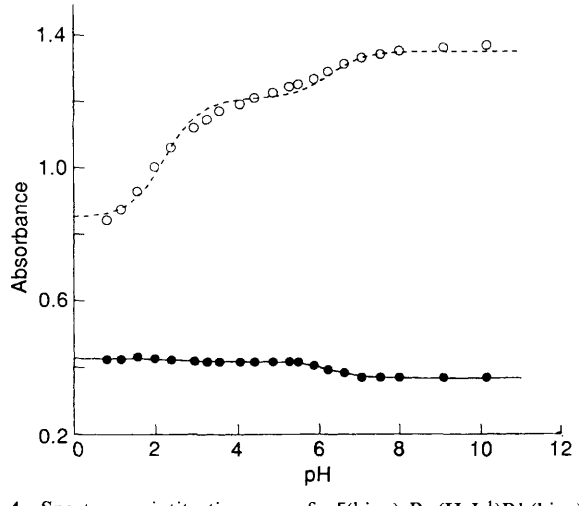

Fig. 4 Spectroscopic titration curves for $[(bipy)_2Ru(H_2L^1)Rh(bipy)_2][ClO_4]_5$ (6.6×10^{-5} mol dm^{-3}) of absorbance at 400 (○) and 461 nm (●) *vs.* pH in MeCN–buffer (1 : 1 v/v)

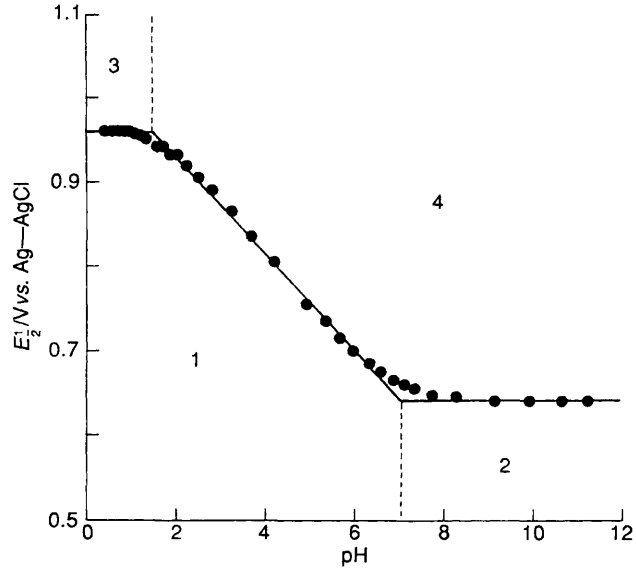

Fig. 5 Plot of the oxidation potential $E_{\frac{1}{2}}$ *vs.* pH for $[Ru(bipy)_2(H_2L^1)][ClO_4]_2$ in MeCN–buffer (1 : 1 v/v) at 20 °C. Species: 1, $[Ru^{II}(H_2L^1)]^{2+}$; 2, $[Ru^{II}(HL^1)]^{+}$; 3, $[Ru^{III}(H_2L^1)]^{3+}$; 4, $[Ru^{III}(HL^1)]^{2+}$

where K_1 and K_2 are the acid-dissociation constants of the ruthenium-(II) and -(III) states, respectively. The pH dependence

$$[Ru^{II}(bipy)_2(H_2L^1)]^{2+} \underset{K_1}{\overset{H^+}{\rightleftharpoons}} [Ru^{II}(bipy)_2(HL^1)]^{+}$$
$$E_1^\circ \downarrow e^- \qquad E_2^\circ \downarrow e^-$$
$$[Ru^{III}(bipy)_2(H_2L^1)]^{3+} \underset{K_2}{\overset{H^+}{\rightleftharpoons}} [Ru^{III}(bipy)_2(HL^1)]^{2+}$$

Scheme 3

$$\begin{array}{ccccc}
[Ru^{II}(H_2L^1)Os^{II}]^{4+} & \underset{K_{11}}{\overset{H^+}{\rightleftharpoons}} & [Ru^{II}(HL^1)Os^{II}]^{3+} & \underset{K_{12}}{\overset{H^+}{\rightleftharpoons}} & [Ru^{II}(L^1)Os^{II}]^{2+} \\
E_1^\circ \downarrow e & & E_3^\circ \downarrow e & & E_5^\circ \downarrow e \\
[Ru^{II}(H_2L^1)Os^{III}]^{5+} & \underset{K_{21}}{\overset{H^+}{\rightleftharpoons}} & [Ru^{II}(HL^1)Os^{III}]^{4+} & \underset{K_{22}}{\overset{H^+}{\rightleftharpoons}} & [Ru^{II}(L^1)Os^{III}]^{3+} \\
E_2^\circ \downarrow e & & E_4^\circ \downarrow e & & E_6^\circ \downarrow e \\
[Ru^{III}(H_2L^1)Os^{III}]^{6+} & \underset{K_{31}}{\overset{H^+}{\rightleftharpoons}} & [Ru^{III}(HL^1)Os^{III}]^{5+} & \underset{K_{32}}{\overset{H^+}{\rightleftharpoons}} & [Ru^{III}(L^1)Os^{III}]^{4+}
\end{array}$$

Scheme 4

of $E_{\frac{1}{2}}$ in Scheme 3 can be expressed by equation (1);[15] where $E_{\frac{1}{2}}^\circ$ is

$$E_{\frac{1}{2}} = E_{\frac{1}{2}}^\circ + \frac{RT}{F} \ln \frac{[H^+] + K_1}{[H^+] + K_2} \quad (1)$$

the half-wave potential of $[Ru(bipy)_2(H_2L^1)]^{2+/3+}$ at pH 0. Given $E_{\frac{1}{2}}^1$ and K_1, a non-linear regression analysis of the Ru^{II}–Ru^{III} redox potentials has been performed.

According to the analysis of the $E_{\frac{1}{2}}$ *vs.* pH diagram, the potential for the monodeprotonated state, $E_2^\circ = 0.64$ V, and the acid dissociation constant for the ruthenium(III) oxidation state, $pK_2 = 1.6$ (see Scheme 3 and Table 2). The pK_a value for the ruthenium(III) state is much smaller than that of Ru^{II}, which reflects the stronger electron-withdrawing properties of the former. The corresponding mononuclear osmium complex behaves in the same manner with values of $pK_1 = 6.7$, $pK_2 = 2.4$, $E_1^\circ = 0.59$ and $E_2^\circ = 0.34$ V *vs.* Ag–AgCl. On the other hand, the rhodium(III) mononuclear complex shows no oxidation waves up to +1.5 V *vs.* Ag–AgCl.

(*b*) *Dinuclear complexes.* The cyclic voltammogram of heterodinuclear $[(bipy)_2Ru(H_2L^1)Os(bipy)_2]^{4+}$ in MeCN–buffer 1:1 v/v) exhibits two oxidation waves at $E_1^\circ = +0.365$ and $E_2^\circ = +0.710$ V *vs.* Ag–Cl at pH 7.10. Coulometry indicated two sequential one-electron processes. The first can be assigned to the Os^{II}–Os^{III} couple and the second to the Ru^{II}–Ru^{III} couple by comparison with the oxidation potentials of each ruthenium and osmium mononuclear unit. These couples also show a pH dependence of $E_{\frac{1}{2}}$ (Fig. 6). The Os^{II}–Os^{III} couple is independent of pH below 2.8 and above 6.9. Over the range pH 2.8–5.6 and 6.4–6.9, the $E_{\frac{1}{2}}$ value decreases linearly with increasing pH with a slope of −60 mV per pH unit. At 5.6 < pH < 6.4, the slope of $E_{\frac{1}{2}}$ *vs.* pH is again independent of pH. A similar pH dependence for the Ru^{II}–Ru^{III} couple was observed in the region examined (see Fig. 6). From the results $[(bipy)_2Ru^{II}(H_2L^1)Os^{II}(bipy)_2]^{4+}$, $[(bipy)_2Ru^{II}(H_2L^1)Os^{III}(bipy)_2]^{5+}$ and $[(bipy)_2Ru^{III}(H_2L^1)Os^{III}(bipy)_2]^{6+}$ each possess two macroscopic acid–base equilibria (Scheme 4).Under these macroscopic acid–base equilibria, the $E_{\frac{1}{2}}$ of the Ru^{II}–Os^{III}/Ru^{II}–Os^{II} couple can be expressed by equation (2):[15] where $E_{\frac{1}{2}}^\circ$ is the standard redox potential of the $[Ru^{II}(H_2L^1)Os^{III}]^{5+}$–$[Ru^{II}(H_2L^1)Os^{II}]^{4+}$ couple at pH 0, n represents the numbers of electrons (here 1), and α_{ox} and α_{red} are as in equations (3) and (4) where K_{11} to K_{22} represent the macroscopic acid-dissociation constants in Scheme 4. According to equations (2)–(4), a non-linear regression fit for the $E_{\frac{1}{2}}$ *vs.* pH profile provides the pK_a values for Ru^{II}–Os^{II} and Ru^{II}–Os^{III} states. Similarly, the $[Ru^{III}(H_2L^1)Os^{III}]^{6+}$–$[Ru^{II}(H_2L^1)Os^{III}]^{5+}$ redox couple has been analysed. As a result, the self-consistent pK_a values are 5.6 and 6.9 for Ru^{II}–Os^{II}, 2.8 and 6.4 for the mixed-valence Ru^{II}–Os^{III}, and 1.4 and 2.8 for Ru^{III}–Os^{III} state, respectively. From the microscopic viewpoint of the proton-coupled electron-transfer reaction, the tautomeric monoprotonated species for different metal oxidation states can be considered with respect to the monoprotonation site in Scheme 5. Owing to the large pK_a difference for the mixed-valence Ru^{II}–Os^{III} complex, the deprotonation is supposed to occur mainly at the osmium(III) site. However, we could determine only the macroscopic pK_a values in the present study. Thus, the molar ratios of the tautomeric forms in solution could not be determined quantitatively (Scheme 5).

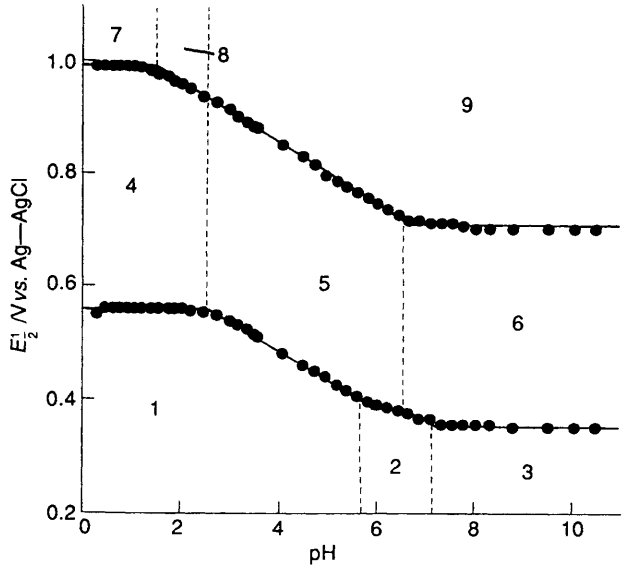

Fig. 6 Plots of the oxidation potentials $E_{\frac{1}{2}}^1$ and $E_{\frac{1}{2}}^2$ *vs.* pH for $[(bipy)_2Ru(H_2L^1)Os(bipy)_2][ClO_4]_2$ in MeCN–buffer (1:1 v/v) at 20 °C. Species: 1, $[Ru^{II}(H_2L^1)Os^{II}]^{4+}$; 2, $[Ru^{II}(HL^1)Os^{II}]^{3+}$; 3, $[Ru^{II}(L^1)Os^{II}]^{2+}$; 4, $[Ru^{II}(H_2L^1)Os^{III}]^{5+}$; 5, $[Ru^{II}(HL^1)Os^{III}]^{4+}$; 6, $[Ru^{II}(L^1)Os^{III}]^{3+}$; 7, $[Ru^{III}(H_2L^1)Os^{III}]^{6+}$; 8, $[Ru^{III}(HL^1)Os^{III}]^{5+}$; 9, $[Ru^{III}(L^1)Os^{III}]^{4+}$

$$E_{\frac{1}{2}} = E_{\frac{1}{2}}^\circ + \frac{RT}{F} \ln \frac{\alpha_{red}}{\alpha_{ox}} \quad (2)$$

$$\alpha_{ox} = 1 + \frac{K_{21}}{[H^+]} + \frac{K_{21}K_{22}}{[H^+]^2} \quad (3)$$

$$\alpha_{red} = 1 + \frac{K_{11}}{[H^+]} + \frac{K_{11}K_{12}}{[H^+]^2} \quad (4)$$

The oxidation of heterodinuclear $[(phen)Ru(H_2L^1)Ru(dmbipy)_2][ClO_4]_4$ occurs first at the $Ru(dmbipy)_2$ moiety, and then at the $Ru(phen)_2$ moiety. However, the protonation site of the HL^1 bridging ligand in the monoprotonated complex may be predominantly at the $Ru(dmbipy)_2$ moiety because of the greater electron-donating ability of the dmbipy ligand relative to phen. A quantitative discussion is not possible.

The cyclic voltammogram of $[(bipy)_2Ru(H_2L^1)Rh(bipy)_2]^{5+}$ in MeCN–buffer (1:1 v/v) shows only one oxidation wave, involving a one-electron process confirmed by coulometry. Furthermore, oxidative spectroelectrochemistry at +1.3 V (*vs.* Ag–AgCl) reveals that the m.l.c.t. band centred at 460 nm disappeared completely and a small l.m.c.t. band around 700 nm appeared. These results confirmed that the oxidation at the $Ru(bipy)_2$ moiety proceeded as a Ru^{II}–Ru^{III} couple. Fig. 7 shows the plot of $E_{\frac{1}{2}}$ *vs.* pH. The oxidation potentials are pH

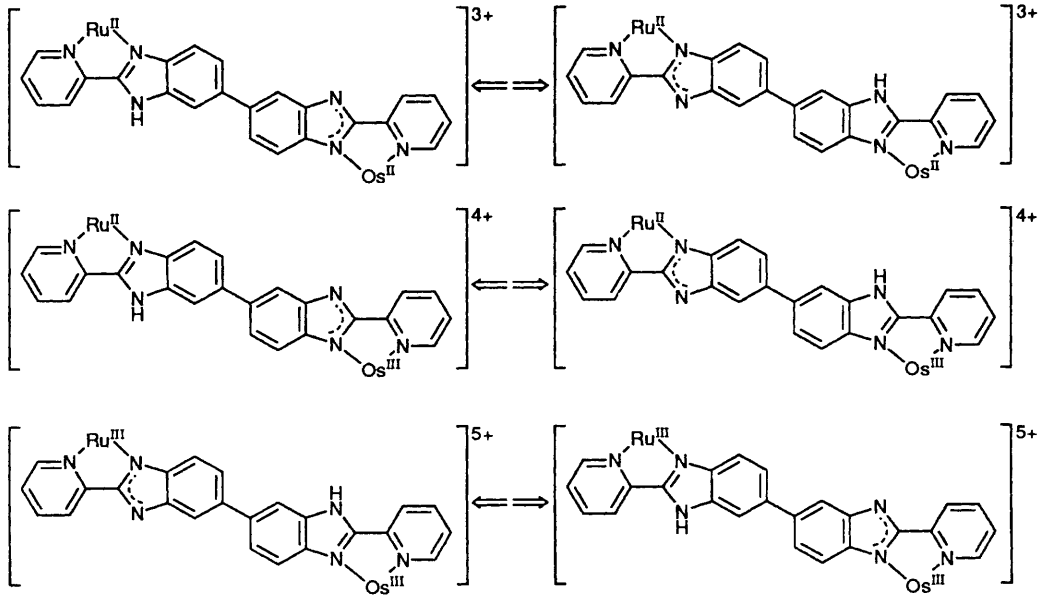

Scheme 5

independent in the pH < 1.4 and > 6.7 regions. Over the range 1.4 < pH < 6.7, the plot is linear with a slope of 54 mV, which is consistent with a one-electron one-proton process. Although the dibasic behaviour of the Ru^{II}–Rh^{III} complex is established by the spectrophotometric measurements described in the previous section, a clear break point was not observed at 1.4 < pH < 6.7. This means that the second acid dissociation of the Ru^{III}–Rh^{III} state occurs very close to the first acid dissociation of the Ru^{II}–Rh^{III} state ($pK_{11} \approx pK_{22}$). Thus, the electrode process can be described in Scheme 6 involving redox and acid–base equilibria. The pK_a data and half-wave potential at pH 0 are summarized in Table 2, which reveals the following relation: $pK_{31} < pK_{21} < pK_{32} \ll pK_{11} < pK_{22} < pK_{12}$.

Effect of the Metal and its Oxidation State on pK_a.—The oxidation potential is shifted to most negative values (≈0.3 V) upon deprotonation, which means that the electron-donating property of the bridging L^1 ligand markedly increases. The pK_a value of the mononuclear metal(II) complexes is about 4–5 pH units higher than that of the metal(III) complexes (M = Ru, Os or Rh). This difference appears to be maintained even in the dinuclear complexes, where two pK_a values are present. Therefore, the following tendency is revealed for the pK_a values of the mono- and di-nuclear complexes; $Os^{II} < Ru^{II}$, $Os^{III} > Ru^{III}$ and $M^{II} \gg M^{III}$ (M = Ru or Os). When the second metal site is redox inactive in the dinuclear complex it acts as a simple electron-withdrawing or -donating substituent. This suggests that the pK_a value for the dinuclear complex can be tuned by selecting the second metal ion.

Characteristics of the Bridging H_2L^1 *Ligand.*—The compound H_2L^1 has stronger donor and weaker acceptor properties compared to those of bipy. Its electron-donating power can be tuned by means of the proton equilibria. The absorption maxima and oxidation potential remained almost unchanged as the mononuclear complex changed into the dinuclear one. From this result the interaction between the two co-ordination sites seems to be relatively small even through the π–π* transition of H_2L^1 shifts to longer wavelength compared to that of HL^3. Recently, complexes of Ru and Os containing L^2 have been reported, where L^2 is a stronger donor and weaker acceptor.[3i] In complexes of L^2 the interaction between two metal ions is relatively strong, although the deprotonation state has not been reported in detail. No solution pH dependence of the oxidation potential has been reported so far. Since L^2 is a

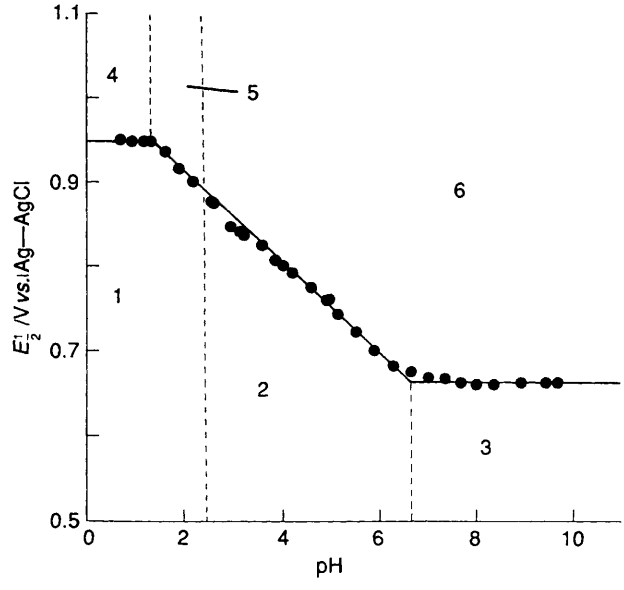

Fig. 7 Plots of the oxidation potentials $E_{\frac{1}{2}}$ *vs.* pH for $[(bipy)_2Ru(H_2L^1)Rh(bipy)_2][ClO_4]_5$ in MeCN–buffer (1:1 v/v) at 20 °C. Species: 1, $[Ru^{II}(H_2L^1)Rh^{III}]^{5+}$; 2, $[Ru^{II}(HL^1)Rh^{III}]^{4+}$; 3, $[Ru^{II}(L^1)Rh^{III}]^{3+}$; 4, $[Ru^{III}(H_2L^1)Rh^{III}]^{6+}$; 5, $[Ru^{III}(HL^1)Rh^{III}]^{5+}$; 6, $[Ru^{III}(L^1)Rh^{III}]^{4+}$

monobasic acid, the possibility of redox and pK_a tuning can be expected by changing the solution pH. However, the pK_a values of co-ordinated L^2 are relatively low,[3i] so strongly acidic conditions will be needed. On the other hand, H_2L^1 acts as a dibasic acid, and the pK_a values of co-ordinated benzimidazoles are around neutral pH. Furthermore, the protonation site and oxidation potential can easily be altered by appropriate selection of the solution pH or the second metal ion.

A shift of the m.l.c.t. band to longer wavelengths and a positive shift in the oxidation potential compared to those of mononuclear complexes have been reported when the latter contains a π-accepting ligand such as L^4, L^5 or L^6 and forms a dinuclear complex.[3c,f,o,q] In contrast, the m.l.c.t. band and the oxidation potential for H_2L^1 complexes remain unaltered on changing from the mono- to the di-nuclear complex. Judging from the m.l.c.t. band energy and redox potentials, the π*-

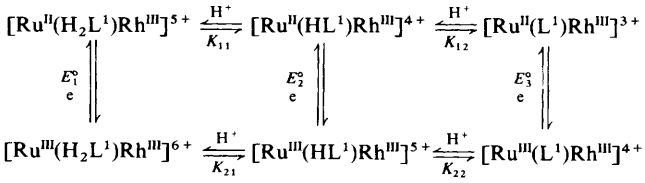

Scheme 6

orbital energies of the bridging ligand decrease in the order L^2 > bipy ≥ H_2L^1 > L^4 > L^6 > L^5.

Conclusion

The bridging H_2L^1 ligand enables the dinuclear complex to act as a diprotic acid, while the mononuclear complex acts not only as a monoprotic acid but also as a monoprotic base. With increasing pH the oxidation potential of the complexes is shifted to more negative values, accompanied by deprotonation. In the heterodinuclear complex the proton transfer concomitant with the redox behaviour depends on both the redox activity of the second metal ion and the oxidation state of the metal ion. Since the proton transfer can be regarded as the trigger to changing the electronic structure of the complex, a desired potential difference can be generated by the proton-transfer equilibria at the specific site through appropriate selection of the combination of the metal ions and peripheral ligands. For example, the diprotonated $[(bipy)_2Ru(H_2L^1)Rh(bipy)_2]^{5+}$ is non-emissive due to the intramolecular electron transfer from excited Ru to Rh; however, emission was observed in the monoprotonated state.[16] This observed emissive switching can be rationalized by the preferential deprotonation at the rhodium(III) site, accompanying the negative potential shift in the reduction potential at this site. In conclusion, the introduction of asymmetry can provide not only a potential difference but also a preferential protonation site in dinuclear complexes.

Experimental

Materials.—3,3′-Diaminobenzidine (Tokyo Kase) and pyridine-2-carboxylic acid (Nakarai) were used as supplied. Tetra-*n*-butylammonium tetrafluoroborate was prepared by standard techniques,[17] recrystallized three times from ethanol–water mixtures and then ethyl acetate–pentane, and vacuum dried at 70 °C for 12 h. Acetonitrile was dried twice over phosphorus pentaoxide and then distilled over CaH_2 under nitrogen. The water used in the measurements was deionized and then purified in a Milipore Milli-Q apparatus. All other chemicals were of analytical grade, and used as supplied. Buffer systems and the pH ranges employed were as follows: $HClO_4$–$NaClO_4$, pH 0–2; Robinson–Britton buffer, pH 2–11.[18]

Preparations.—The starting complexes $[Ru(bipy)_2Cl_2]\cdot 2H_2O$, $[Ru(dmbipy)_2Cl_2]\cdot 2H_2O$, $[Ru(phen)_2Cl_2]$, $[Rh(bipy)_2Cl_2]Cl$, $[Rh(phen)_2Cl_2]Cl$, and $[Os(bipy)_2Cl_2]$, were prepared by the literature methods.[19] The dinucleating compound H_2L^1 was prepared by the previous method.[7] **CAUTION:** Perchlorate salts are potentially explosive. Although no detonation tendencies have been observed, caution is advised and handling of only small quantities is recommended.

Mononuclear complexes. $[Ru(bipy)_2(H_2L^1)][ClO_4]_2\cdot 5H_2O$. A suspension of *cis*-$[Ru(bipy)_2Cl_2]\cdot 2H_2O$ (0.79 g, 1.63 mmol) was dissolved in ethanol–water (1:1 v/v, 40 cm^3) under reflux for 1 h. To the resulting solution was added H_2L^1 (0.70 g, 1.8 mmol). Refluxing was continued for 5 h, during which the colour gradually turned red. The solution was concentrated to 20 cm^3 and then filtered. Addition of a saturated aqueous $NaClO_4$ solution effected precipitation of the complex. The product was purified by column chromatography on SP Sephadex C-25 with acetonitrile–Britton–Robinson buffer (1:1 v/v, pH 5.0) as eluent. The second band was collected. Yield 0.81 g (45.4%) (Found: C, 48.75; H, 3.25; N, 12.25. Calc. for $C_{44}H_{32}Cl_2N_{10}O_8Ru\cdot 5H_2O$: C, 48.45; H, 3.90; N, 12.85%).

$[Ru(dmbipy)_2(H_2L^1)][ClO_4]_2$. The complex *cis*-$[Ru(dmbipy)_2Cl_2]\cdot 2H_2O$ (0.89 g, 1.65 mmol) was suspended in ethanol–water (1:1 v/v), and heated until dissolution was complete (about 1 h). Solid H_2L^1 (0.64 g, 1.65 mmol) was added. The mixture was refluxed for 6 h, during which time it became dark red. The solvent was evaporated to dryness and the residue dissolved in the minimum of methanol, then loaded on a Sephadex LH-20 column (3 × 50 cm) and eluted with methanol. The second orange band was collected, and concentrated to about 30 cm^3. To the resulting solution was added $NaClO_4$ (1 g, 7.1 mmol) in water (5 cm^3). A red-orange precipitate was formed, which was recrystallized from methanol–water (5:1 v/v). 0.69 g (39% yield) (Found: C, 54.25; H, 4.00; N, 13.10. Calc. for $C_{48}H_{40}Cl_2N_{10}O_8Ru$: C, 54.55; H, 3.80; N, 13.25%).

$[Os(bipy)_2(H_2L^1)][ClO_4]_2\cdot 5H_2O$. A mixture of $[Os(bipy)_2Cl_2]\cdot 2H_2O$ (0.4 g, 0.70 mmol) and H_2L^1 (0.27 g, 0.70 mmol) in ethanol–water (1:1 v/v, 40 cm^3) was refluxed for 12 h. Ethanol was removed *in vacuo*, and the resulting dark yellow solution was filtered. Sodium perchlorate (0.5 g, 3.6 mmol) in water (5 cm^3) was added to the filtrate. The black precipitate was filtered off and recrystallized from methanol–water (10:1 v/v), 0.5 g (63% yield) (Found: C, 45.50; H, 3.35; N, 11.10. Calc. for $C_{44}H_{32}Cl_2N_{10}O_8Os\cdot 5H_2O$: C, 45.50; H, 3.45; N, 12.05%).

$[Rh(bipy)_2(H_2L^1)][ClO_4]_3\cdot 4H_2O$. A mixture of *cis*-$[Rh(bipy)_2Cl_2]Cl$ (0.50 g, 1 mmol) and H_2L^1 (0.41 g, 1.1 mmol) in ethanol–water (3:1 v/v, 60 cm^3) was refluxed with stirring for 24 h. The progress of the reaction was monitored by UV spectroscopy until the absorbance of the band around 370 nm was constant. The solution gradually turned yellowish orange. It was concentrated to 10 cm^3, and then filtered in order to remove the excess of unreacted H_2L^1. Addition of a saturated aqueous $NaClO_4$ solution to the filtrate effected precipitation of the complex. The product was purified by recrystallization from ethanol–water. Yield 0.70 g (58%) (Found: C, 45.10; H, 3.40; N, 11.90. Calc. for $C_{44}H_{32}Cl_3N_{10}O_{12}Rh\cdot 4H_2O$: C, 45.00; H, 3.45; N, 11.95%).

$[Rh(phen)_2(H_2L^1)][ClO_4]_3\cdot 4H_2O$. This compound was prepared following the same procedures as used for the Rh(bipy) analogue, employing *cis*-$[Rh(phen)_2Cl_2]Cl$ (Yield 77%) (Found: C, 47.75; H, 3.25; N, 11.55. Calc. for $C_{48}H_{32}Cl_3N_{10}O_{12}Rh\cdot 4H_2O$: C, 47.20; H, 3.30; N, 11.45%).

Dinuclear complexes. $[(bipy)_2Ru(H_2L^1)Os(bipy)_2][ClO_4]_4\cdot 4H_2O$. The complex $[Ru(bipy)_2Cl_2]$ (0.13 g, 0.26 mmol) was dispersed in ethylene glycol (30 cm^3) and stirred with heating at 120 °C for 2 h. To this brown solution was added solid $[Os(bipy)_2(H_2L^1)][ClO_4]_2$ (0.3 g, 0.26 mmol), and the solution refluxed for 6 h. The resulting mixture was poured into an aqueous solution of $NaClO_4$ (1.0 g, 8.2 mmol), precipitating the desired complex. The product was filtered off and purified by SP Sephadex C-25 column chromatography with acetonitrile–Britton–Robinson buffer (1:1 v/v, pH 8.5) as eluent. The dark brown third band was collected, followed by evaporation of the solvent. The dark black residue was recrystallized from methanol–water (5:1 v/v). Yield 0.14 g (31%) (Found: C, 43.50;

H, 2.80; N, 11.10. Calc. for $C_{64}H_{56}Cl_4N_{14}O_{20}OsRu\cdot4H_2O$: C, 43.30; H, 3.20; N, 11.05%).

$[(bipy)_2Ru(H_2L^1)Rh(bipy)_2][ClO_4]_5\cdot4H_2O$. The complex $[Ru(bipy)_2Cl_2]$ (0.23 g, 0.47 mmol) was dispersed in ethylene glycol (30 cm^3) and stirred with heating at 120 °C for 2 h. To this brown solution was added solid $[Rh(bipy)_2(H_2L^1)][ClO_4]_2$ (0.47 g, 0.42 mmol), and the solution refluxed for 3 h. The reaction mixture was poured into an aqueous solution of $NaClO_4$ (1.0 g, 8.2 mmol), precipitating the desired complex. The product was filtered off and purified by SP Sephadex C-25 column chromatography with acetonitrile–Britton–Robinson buffer (1 : 1 v/v, pH 8.5 + 0.1 mol dm^{-3} $NaClO_4$) as eluent. The dark orange third band was collected, followed by evaporation of the solvent. The orange residue was recrystallized from methanol–water (5 : 1 v/v). Yield 0.34 g (41%) (Found: C, 43.80; H, 3.00; N, 11.35. Calc. for $C_{64}H_{48}Cl_5N_{14}O_{20}RhRu\cdot2H_2O$: C, 43.90; H, 3.00; N, 11.20%).

$[(dmbipy)_2Ru(H_2L^1)Ru(phen)_2][ClO_4]_5\cdot5H_2O$. The complex $[Ru(phen)_2Cl_2]$ (0.15 g, 0.28 mmol) was dispersed in ethylene glycol (30 cm^3) and stirred with heating at 120 °C for 2 h. To this brown solution was added solid $[Ru(dmbipy)_2(H_2L^1)][ClO_4]_2$ (0.3 g, 0.26 mmol), and the solution refluxed for 6 h. The resulting reaction mixture was poured into an aqueous solution of $NaClO_4$ (1.0 g, 8.2 mmol), precipitating the desired complex. The product was filtered off and purified by SP Sephadex C-25 column chromatography with acetonitrile–Britton–Robinson buffer (1 : 1 v/v, pH 8.5 + 0.1 mol dm^{-3} $NaClO_4$) as eluent. The dark orange third band was collected, followed by evaporation of the solvent. The orange residue was recrystallized from methanol–water (5 : 1 v/v). Yield 0.20 g (39%) (Found: C, 47.70; H, 3.50; N, 10.70. Calc. for $C_{72}H_{56}Cl_4N_{14}O_{16}Ru_2\cdot4H_2O$: C, 47.85; H, 3.70; N, 10.85%).

$[(phen)_2Rh(H_2L^1)Rh(phen)_2][ClO_4]_6\cdot2H_2O$. A mixture of $[Rh(phen)_2Cl_2]Cl$ (0.33 g, 0.57 mmol) and H_2L^1 (0.10 g, 0.26 mmol) in ethanol–water (4 : 1 v/v, 50 cm^3) was heated under reflux for 24 h, during which time it changed from pale yellow to orange. The solvent was evaporated to half-volume, and the resulting solution was filtered. To the filtrate aqueous $NaClO_4$ (0.8 g, 5.7 mmol) was added. The yellow precipitate was purified by recrystallization from ethanol–water. Yield 0.35 (70%) (Found: C, 44.05; H, 2.70; N, 9.85. Calc. for $C_{72}H_{48}Cl_6N_{14}O_{24}Rh_2\cdot2H_2O$: C, 44.40; H, 2.70; N, 10.05%).

Physical Measurements.—Electronic spectra were obtained on a Hitachi U-3210 spectrophotometer from 200 to 850 nm and a Hitachi 3400 spectrophotometer from 800 to 2600 nm. The pH measurements were made with a TOA model HM-20E pH meter standardized with buffers of pH 4.01 and 6.86 (at 25 °C). A 50% acetonitrile–water mixture was employed because of the solubility limit of the present complexes in pure aqueous solution, particularly at higher pH. The pH meter readings in this mixture are referred to as 'apparent' pH unless otherwise stated. Spectrophotometric titrations were performed in acetonitrile–water (1 : 1 v/v) solution, as described previously.[7] The osmium(III) oxidation state was generated by chemical oxidation of the osmium complexes with $NOBF_4$.

Electrochemical measurements were made at 20 °C with a Yanagimoto P-1100 Polarographic Analyzer equipped with a Watanabe WX-4401 x-y recorder. The working electrode was a glassy-carbon electrode and the auxiliary electrode was a platinum plate. The reference electrode was a BAS RE-1 Ag–AgCl electrode. It was calibrated by the internal ferrocene–ferrocenium couple under the same conditions. Spectroelectrochemistry was performed by using a platinum minigrid (80 mesh) working electrode in the thin-layer cell designed originally by Lexa *et al.*[20] The cell was located directly in the spectrophotometer, and the absorption change was monitored during the electrolysis. The pK_a values for various oxidation states of the mono- and di-nuclear complexes can be obtained by analysing plots of the potential $E_{\frac{1}{2}}$ *vs.* pH (Pourbaix diagram). In a reversible redox system the midpoint between the cathodic and anodic peak potentials can be regarded as the reversible half-wave potential ($E_{\frac{1}{2}}$).

Acknowledgements

This work was supported by a Grant-in-Aid for Scientific Research (No. 02640474 and 04453045) from the Ministry of Education, and a basic science grant from the Sumitomo Foundation.

References

1 (*a*) V. Balzani, L. Moggi and F. Scandola, *Supramolecular Photochemistry*, ed. V. Balzani, Reidel, Dordrecht, 1987, p. 1; (*b*) V. Balzani and F. Scandola, *Supramolecular Photochemistry*, Ellis Horwood, Chichester, 1991.

2 S. Woitellier, J. P. Launay and C. W. Spangler, *Inorg. Chem.*, 1989, **28**, 758; J. P. Launay, *Molecular Electronic Devices II*, ed. F. L. Carter, Marcel Dekker, New York, 1987, p. 39; J. J. Hopfield, J. N. Onuchic and D. N. Beratan, *Science*, 1988, **241**, 817; Y. Kim and C. M. Lieber, *Inorg. Chem.*, 1989, **28**, 3990; S. Serroni, G. Denti, S. Campagna, A. Juris, M. Ciano and V. Balzani, *Angew. Chem., Int. Ed. Engl.*, 1992, **31**, 1493.

3 (*a*) T. Ohno, *Prog. React. Kinet.*, 1988, **14**, 219; (*b*) F. Scandola, C. A. Bignozzi, C. Chiorboli, M. T. Indelli and M. A. Rampi, *Coord. Chem. Rev.*, 1990, **97**, 299; (*c*) J. D. Petersen, *Supramolecular Photochemistry*, ed. V. Balzani, Reidel, Dordrecht, 1987, p. 135; (*d*) J.-M. Lehn, *Supramolecular Photochemistry*, ed. V. Balzani, Reidel, Dordrecht, 1987, p. 29; (*e*) C. A. Bignozzi, S. Roffia, C. Chiorboli, J. Davila, M. T. Indelli and F. Scandola, *Inorg. Chem.*, 1989, **28**, 4350; (*f*) D. P. Rillema, R. W. Callahan and K. B. Mack, *Inorg. Chem.*, 1982, **21**, 2589; (*g*) S. Ernst and W. Kaim, *Inorg. Chem.*, 1989, **28**, 1520; (*h*) L. De Cola, P. Belser, F. Ebmeyer, F. Barigelletti, F. Vogtle, A. von Zelewsky and V. Balzani, *Inorg. Chem.*, 1990, **29**, 495; (*i*) R. Hage, A. H. J. Dijkhuis, J. D. Haasnoot, R. Prins, J. Reedijk, B. E. Buchana and J. G. Vos, *Inorg. Chem.*, 1988, **27**, 2185; (*j*) J. R. Shaw, R. T. Webb and R. H. Schmehl, *J. Am. Chem. Soc.*, 1990, **112**, 1117; (*k*) K. S. Schanze, G. A. Neyhart and T. J. Meyer, *J. Phys. Chem.*, 1986, **90**, 2182; (*l*) J. C. Curtis, J. S. Bernstein and T. J. Meyer, *Inorg. Chem.*, 1985, **24**, 385; (*m*) T. J. Meyer, *Prog. Inorg. Chem.*, 1983, **30**, 389; (*n*) V. Balzani and F. Scandola, *Photoinduced Electron Transfer. Part D*, eds. M. A. Fox and M. Chanon, Elsevier, New York, 1988, p. 148; (*o*) W. R. Murphy, K. J. Brewer, G. Gettliffe and J. D. Petersen, *Inorg. Chem.*, 1989, **28**, 81; (*p*) D. P. Rillema, R. Sahai, P. Matthews, A. K. Edwards, R. J. Shaver and L. Morgan, *Inorg. Chem.*, 1990, **29**, 167; (*q*) Y. Fuchs, S. Lofters, T. Dieter, W. Shi, R. Morgan, T. C. Strekas, H. D. Gafney and A. D. Baker, *J. Am. Chem. Soc.*, 1987, **109**, 2691; (*r*) M. Hunziger and A. Ludi, *J. Am. Chem. Soc.*, 1977, **99**, 7370; (*s*) M. Furue, T. Yoshidzumi, S. Kinoshita, T. Kushida, S. Nozakura and M. Kamachi, *Bull. Chem. Soc. Jpn.*, 1991, **64**, 1632; (*t*) A. J. Downard, G. E. Honey, L. F. Phillips and P. J. Steel, *Inorg. Chem.*, 1991, **30**, 2260; (*u*) G. Denti, S. Campagna, S. Serroni, M. Ciano and V. Balzani, *J. Am. Chem. Soc.*, 1992, **114**, 2944; (*v*) M. M. Richter and K. J. Brewer, *Inorg. Chem.*, 1992, **31**, 1594; (*x*) K. Kalyanasundaram and M. K. Nazeeruddin, *J. Chem. Soc., Dalton Trans.*, 1990, 1657; (*y*) C. R. Arana and H. D. Abruna, *Inorg. Chem.*, 1993, **32**, 194; (*z*) K. Kalyanasundaram, *Photochemistry of Polypyridine and Porphyrin Complexes*, Academic Press, London, 1991.

4 T. J. Meyer, *Acc. Chem. Res.*, 1989, **22**, 163; M. A. Fox, *Acc. Chem. Res.*, 1992, **25**, 569; S. Serroni and G. Denti, *Inorg. Chem.*, 1992, **31**, 4251; F. Fagalde and N. Katz, *J. Chem. Soc., Dalton Trans.*, 1993, 571; G. Denti, S. Serroni, S. Campagna, V. Ricevuto and V. Balzani, *Inorg. Chim. Acta*, 1991, **182**, 127; V. Grosshenny and R. Ziessel, *J. Chem. Soc., Dalton Trans.*, 1993, 817; L. M. Vogler, B. Scott and K. J. Brewer, *Inorg. Chem.*, 1993, **32**, 898; J. H. van Diemen, R. Hage, J. G. Haasnoot, H. E. B. Lempers, J. Reedijk, J. G. Vos, L. De Cola, F. Barigelletti and V. Balzani, *Inorg. Chem.*, 1992, **31**, 3518; C. A. Bignozzi, O. Bortolini, C. Chioboli, M. T. Indelli, M. A. Rampi and F. Scandola, *Inorg. Chem.*, 1992, **31**, 172; C. A. Bignozzi, A. Argazzi, C. G. Garcia, F. Scandola, J. R. Schoonover and T. J. Meyer, *J. Am. Chem. Soc.*, 1992, **114**, 8727.

5 E. C. Constable and P. J. Steel, *Coord. Chem. Rev.*, 1989, **93**, 205.

6 M. Haga, T. Matsumura-Inoue and S. Yamabe, *Inorg. Chem.*, 1987, **26**, 4148; D. P. Rillema, R. Sahai, P. Matthews, A. K. Edwards, R. J. Shaver and L. Morgan, *Inorg. Chem.*, 1990, **29**, 167.

7 M. Haga, T. Ano, K. Kano and S. Yamabe, *Inorg. Chem.*, 1991, **30**, 3843.

8 K. Nozaki, M. Haga and T. Ohno, manuscript in preparation.
9 R. D. Feltham and R. G. Hayter, *J. Chem. Soc.*, 1964, 4587.
10 M. Haga, *Inorg. Chim. Acta*, 1983, **75**, 29.
11 T. Ohno, K. Nozaki and M. Haga, *Inorg. Chem.*, 1992, **31**, 548.
12 D. H. W. Carstens and G. A. Crosby, *J. Mol. Spectrosc.*, 1970, **34**, 113.
13 M. F. Hoq and R. E. Shepherd, *Inorg. Chem.*, 1984, **23**, 1851; A. M. Bond and M. Haga, *Inorg. Chem.*, 1986, **25**, 4507.
14 J. Polster and H. Lachmann, *Spectrometric Titrations—Analysis of Chemical Equilibria*, VCH, New York, NY, 1989, ch. 12.
15 W. M. Clark, in *Oxidation–Reduction Potentials of Organic Systems*, Williams & Wilkins, Baltimore, 1960, ch. 4; L. Meites, in *Polarographic Techniques*, 2nd edn., Interscience, New York, 1965, ch. 5.
16 K. Nozaki, T. Ohno and M. Haga, *J. Phys. Chem.*, 1992, **96**, 10880.
17 A. J. Fry and W. E. Britton, in *Laboratory Techniques in Electroanalytical Chemistry*, eds. P. T. Kissinger and W. R. Heineman, Marcel Dekker, New York, 1984, p. 367.
18 H. T. Britton and R. A. Robinson, *J. Chem. Soc.*, 1931, **45**, 1456.
19 P. A. Lay, A. Sargeson and H. Taube, *Inorg. Synth.*, 1986, **24**, 291.
20 D. Lexa, J. M. Saveant and J. Zickler, *J. Am. Chem. Soc.*, 1977, **99**, 2786.

Received 15*th June* 1993; *Paper* 3/03452F